



EUROPEAN  
COMMISSION

Community research

# BELBaR

(Contract Number: 295487)

## DELIVERABLE (D-N°:2.9)

Analysis and characterization of the bentonite gel and colloids  
obtained in erosion tests

Author(s):

**Frank Friedrich, Franz Rinderknecht**  
**KIT-CN/INE**

**Michał Matusiewicz, Veli-Matti Pulkkanen, Markus Olin**  
**VTT Technical Research Centre of Finland Ltd.**

Reporting period: 01/03/12 – 29/02/16

Date of issue of this report: 31/05/2015

Start date of project: **01/03/12**

Duration: 48 Months

<b>Project co-funded by the European Commission under the Seventh Euratom Framework Programme for Nuclear Research &amp; Training Activities (2007-2011)</b>		
<b>Dissemination Level</b>		
<b>PU</b>	Public	X
<b>RE</b>	Restricted to a group specified by the partners of the BELBaR project	
<b>CO</b>	Confidential, only for partners of the BELBaR project	

BELBaR



## DISTRIBUTION LIST

Name	Number of copies	Comments
Christophe Davies (EC)		
BELBaR participants		

## **Deliverable D2.9 – Background and Objectives**

The objective of the BELBaR Work Package 2 is to understand the mechanisms of colloid and gel layer formation during bentonite erosion. A special focus was set on the characterization of the bentonite gel, which is built during the hydration and swelling of the compacted bentonite.

This report summarizes the results from work performed at VTT Technical Research Centre of Finland and KIT-CN/INE during the reporting period from the 1<sup>st</sup> of June 2014 to 31<sup>st</sup> of May 2015.

In the contribution of VTT the influence of preparation parameters on the microstructure of compacted clays is discussed. They used different procedures to obtain water saturated, compacted samples from MX80 bentonite (air dry compacted bentonite saturated with Milli-Q water or 0.1 M NaCl solution, and one bentonite sample presaturated with Milli-Q before compaction). Based on the SAXS results they could show, that these preparation techniques induced differences in the microstructure of the compacted bentonite.

The contribution of KIT-CN/INE contains two parts. In part I the status of the work on the erosion and swelling behavior of FEBEX bentonite is presented and results from erosion experiments are discussed.

In Part II the use of environmental scanning electron microscopy (ESEM) coupled with digital image analysis for the in-situ observation and measurement of the hydration and swelling behavior of Febex bentonite is demonstrated. Isotherms measured on different cation exchanged samples over a broad range of relative humidities between 14 % and 95 % are compared.

### **Report from work performed at VTT**

(Michał Matuszewicz, Veli-Matti Pulkkanen, Markus Olin)

#### **1 Background and Objectives**

Research done at VTT was focusing on the clay microstructure at different conditions of density and saturating water salinity. Purified, homoionic MX-80 bentonite in calcium or sodium form and as received MX-80 were investigated. Additionally a study on sample preparation influence on the microstructure has been conducted.

The goal of this work was to characterize the clay microstructure at the start of the erosion. This is important for understanding the erosion process, as the initial state of the clay should be linked with its swelling properties and the colloid particle generation.

#### **2 Summary**

In the microstructure investigation three types of samples were investigated: purified MX-80 in sodium or calcium form and as received MX-80 bentonite. The parameters varied were dry density and the salinity of the equilibration solution. Analytical methods used for the structure characterization were: small-angle X-ray scattering (SAXS), nuclear magnetic resonance

(NMR), transmission electron microscopy (TEM) and ion exclusion (IE). More details about the sample preparation and the methods used can be found in Matuszewicz et al. [1].

In the investigation of the sample preparation influence on microstructure the samples were prepared from MX-80 clay and SAXS was used to estimate variations of the structure. More detailed description can be found in Matuszewicz et al. [2].

### 3 Results

#### 3.1 Microstructural investigation

The research on the clay microstructure was published in Matuszewicz et al. [1] and described in previous deliverables [3, 4].

#### 3.2 Influence of the sample preparation on the clay micro-structure [2]

##### 3.2.1 Sample preparation

A set of water saturated samples at target densities of 0.7, 1.0, 1.3 and 1.5 g/cm<sup>3</sup> was investigated. Starting point was an as-received powder sample and four different ways of preparation were used:

1. Air-dry clay is compacted to the target density if required and saturated with Milli-Q water in confined volume
2. Air-dry clay is compacted to approximately 1.8 g/cm<sup>3</sup>, saturated with Milli-Q water and let to swell to the target density
3. Air-dry clay is compacted to approximately 1.8 g/cm<sup>3</sup>, saturated with 0.1M NaCl solution and let to swell to the target density
4. Milli-Q water saturated clay at 1.6 g/cm<sup>3</sup> dry density is let to swell to the target density.

The sample preparation methods are schematically shown in the Figure 1.

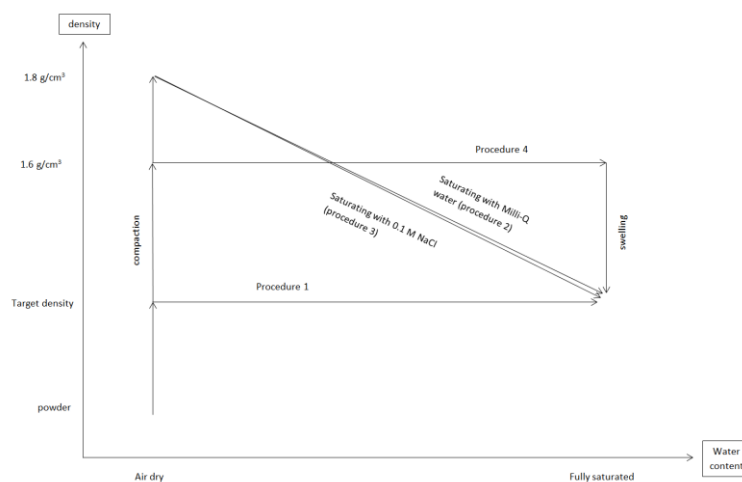


**Figure 1.** Schematic representation of the clay sample preparation method.

0.7

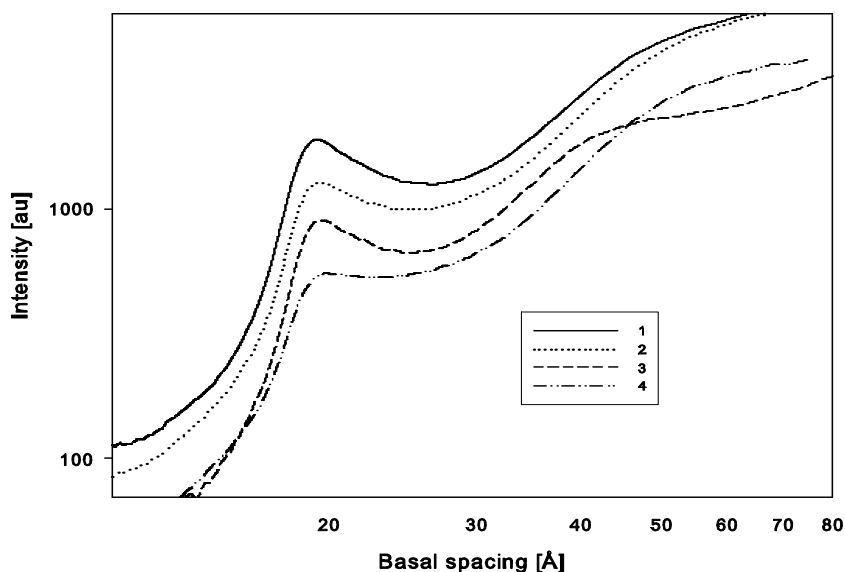


**Figure 2.** X-ray scattering curve of the samples of  $0.7 \text{ g/cm}^3$  dry density. Sample numbers in the legend correspond to the preparation procedures described in the text.

### 3.2.2 SAXS spectra

The small-angle X-ray scattering spectra were used as an indicator of the microstructural variations between the samples. Figures 2 and 3 show examples of scattering curves from samples of the same density made by different preparation procedures.

### 3.2.3 Latest results summary

Differences between the scattering curves were observed for the samples of the same density. The extent of the differences varied between the density sets, being the biggest for the samples of the lowest density.

Results of the sample preparation testing show that different procedures used to obtain water saturated, compacted samples may induce differences in the microstructure. This, in consequence, can influence the results obtained from the erosion tests. However, further systematic work and more thorough testing are needed to understand the relation between different ways of the sample preparation and resulting variations in the microstructure.

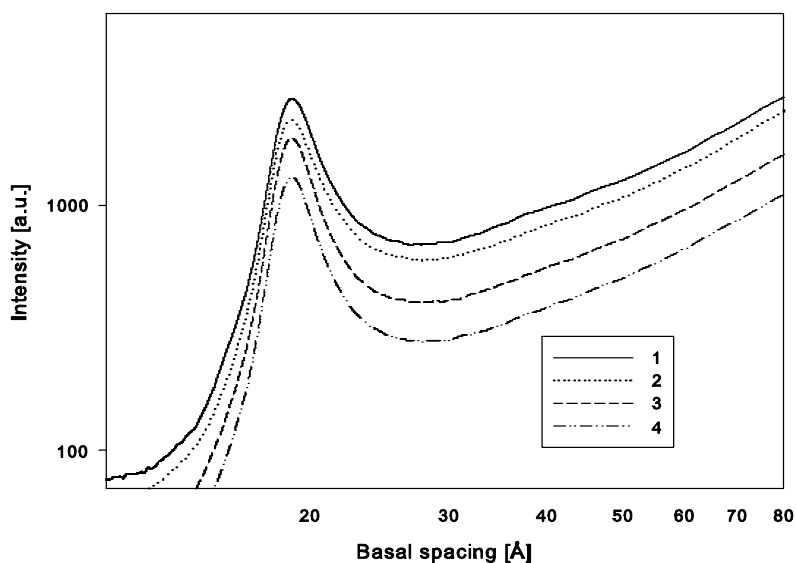


**Figure 3.** X-ray scattering curve of the samples of  $1.3 \text{ g/cm}^3$  dry density. Sample numbers in the legend correspond to the preparation procedures described in the text.

## 4 Conclusions and Next Steps

Only part of the data acquired in the project has been published so far. Publications concerning sodium montmorillonite and MX-80 microstructure will be submitted to publication later this year.

Further research on the influence of the preparation procedures on the sample microstructure can be carried on. More variations of experimental conditions (density, salinity) can be tested and other methods used in our team (e.g. NMR) can be applied. Work done so far considered only MX-80 bentonite but can be expanded also to other clays considered for the spent nuclear fuel disposal.

## References

- [1] M. Matuszewicz, V. Liljeström, K. Pirkkalainen, J.P. Suurinen, A. Root, A. Muurinen, R. Serimaa, M. Olin, "Microstructural investigation of calcium montmorillonite". *Clay Minerals* 48, no. 2 (2013): 267-276
- [2] M. Matuszewicz, V. M. Pulkkanen, M. Olin, "Influence of the sample preparation on bentonite microstructure", submitted to *Clay Minerals*
- [3] Progress Report on the analysis and characterization of the bentonite gel and colloids obtained in erosion tests, Belbar deliverable D2.3, M. Kataja (ed.)
- [4] Progress Report on the analysis and characterization of the bentonite gel and colloids obtained in erosion tests, Belbar deliverable D2.6, F. Friedrich, F. Rinderknecht, M. Kataja, J. Alaraudanjoki, T. Harjupatana, M. Matuszewicz, V.-M. Pulkkanen, M. Olin

# Report from work performed at KIT-CN/INE – Part I

State of the art report of the work on the erosion and swelling behavior of the FEBEX bentonite. (F. Rinderknecht)

## 1. Summary

At KIT-CN/INE the erosion and swelling behavior of the FEBEX bentonite has been investigated. Therefore erosion experiments were conducted in custom-made flow through cells. During the experiments the bentonite swelling pressure was monitored and the colloid concentration and the colloidal size distribution was measured. In this report results of these measurements are presented.

## 2. Set-ups for erosion experiments

At KIT-CN/INE the erosion and swelling behaviour of the FEBEX bentonite has been investigated during erosion experiments conducted in a custom-made flow through cell. Figure 1 shows the set-up of these kind of cells. The housing is made of acrylic glass and has a diameter of 18 cm and an aperture of 1 mm. For the tests compacted FEBEX bentonite rings (inner diameter: 4 cm, outer diameter 8 cm, height: 2.5 cm) were used, which were provided by CIEMAT (initial density:  $1650 \text{ kg/m}^3$ ). The rings were placed in a cavity in the center of the cell and were dry and not presaturated prior to the experiment. Grimsel groundwater was pumped through the cell by a peristaltic pump with an initial flow velocity  $v_{\text{init.}} = 10^{-5} \text{ m/s}$ .

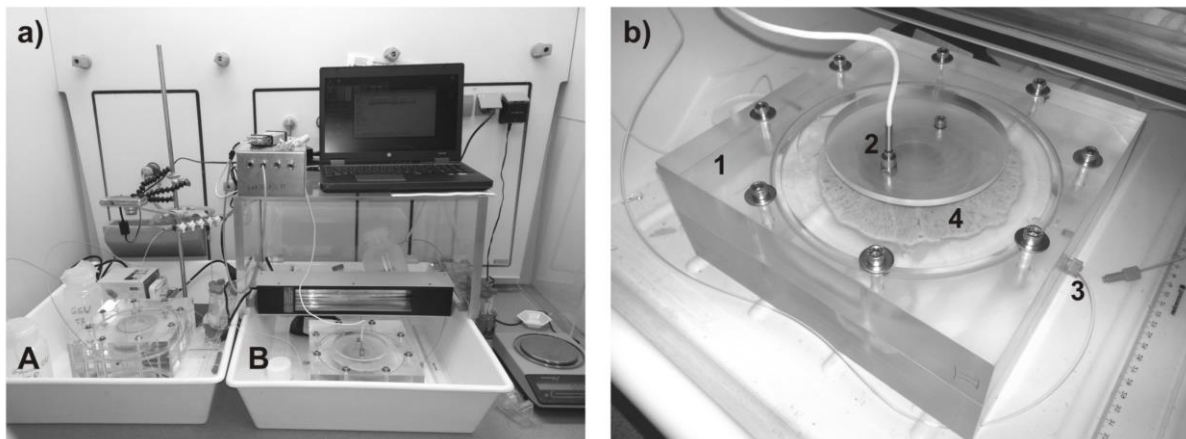


**Figure 1.** a) setup of the erosion experiments. Setup (A) on the left with an experiment for mineralogical characterization of the erosion-“halo”. Setup (B) on the right: long-term erosion experiment equipped with a pressure sensor. b) Setup (B) during the experiment, visible are the acrylic glass housing (1), the pressure sensor (2) with the (dark) bentonite ring beneath, the water inlet (3) and the erosion halo (4).

One erosion setup is used for a long-term experiment (Figure 1b). It is running continuously since October 2013. Thereby the bentonite ring was filled with eight thin glass vials containing 220 mg (synthetic Ni-labelled) montmorillonite (as paste), spiked with 10 mg uranine in each vial as conservative tracer and the homologues Eu, Th, Hf and Tb (25  $\mu\text{g}$  per vial, respectively). Therefore, eight holes were drilled laterally to mount the glass vials. Due to the swelling of the clay the glass vials are supposed to break and release the labelled montmorillonite and associated tracers as well as the conservative tracer. Furthermore this

cell was equipped with a pressure sensor (disynet XP1103-A1-100BG) to monitor the evolution of the bentonite swelling pressure during the experiment (Figure 1, b.2).

### 3. Measurement of swelling pressure

Within the first 24 h after the start of the experiment the swelling pressure rises up to 2.6 MPa (Figure 2a). During the following days the pressure decreases to a constant value between 1.7 to 1.8 MPa implying steady state conditions (Figure 2b). This pressure drop coincides with the bentonite swelling into the 1 mm aperture.

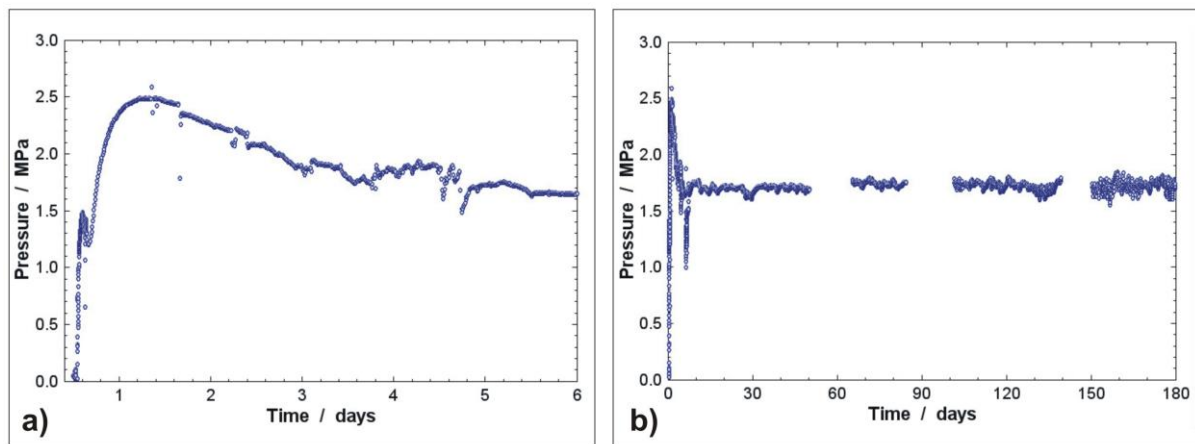


**Figure 2.** Results of pressure measurements over a time period of 180 days.

Water samples of the reactor effluent are taken regularly for analysis of elemental composition, fluorescence, pH, colloid size and concentration. These data are evaluated within the following months. The colloidal size distribution and concentration obtained is depicted in Figure 3.

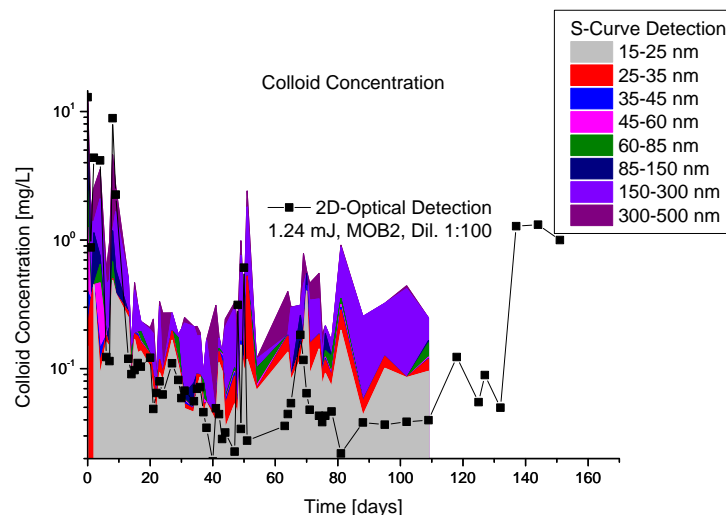


**Figure 3.** Colloidal size distribution measured by s-curve LIBD and MOB2-LIBD.

During the first days of the experiment a high colloid concentration is detected (initially ~10 mg/l) which could be explained by the release of most likely accessory minerals and loosely

aggregates during the initial saturation of the setup followed by a decrease of colloid concentration to values around 0.2 to 1 mg/l after 50 d.

The set-up was moved into an Ar-glovebox in May, 2014 in order to prevent carbonisation. The effluent is sampled continuously and the eroded material is scheduled to be used in radionuclide sorption experiments.

## **Report from work performed at KIT-CN/INE – Part II**

Hydration of FEBEX-Bentonite observed by Environmental Scanning Electron Microscopy (ESEM). (F. Friedrich, D. Schild, and T. Schäfer)  
(Published at CMS workshop lecture series / EUROCLAY2015 special edition)

### **1. Introduction**

During the reporting period the swelling behavior of FEBEX-bentonite was investigated using environmental scanning electron microscopy (ESEM).

This techniques reveals the unique possibility to investigate sensitive and even wet materials (e.g. Donald 1998). Due to its ability to adjust the relative humidity around the sample very precisely, it is an excellent tool for the investigation of the swelling behavior of clays (e.g. Carrier et al. 2013, Montes-H et al. 2003). Thus our focus was set on the in-situ electron microscopic quantification of the swelling of different cation exchanged bentonite samples, which than was compared to the raw material.

### **2. Method**

#### **2.1 Environmental scanning electron microscopy (ESEM) of wet samples**

In this study the fraction  $< 2 \mu\text{m}$  of the FEBEX-bentonite was used, and several cation exchanged samples were produced: Na-, Li-, Sr-exchanged bentonite and one layer charge reduced sample (Li-bentonite heated to 300°C).

All microscopic measurements were carried out in a FEI Quanta 650 environmental scanning electron microscope (ESEM), which was equipped with a gaseous secondary electron detector (GSED). The microscope was operated at 20 kV in wet-mode under varying water vapor pressures between 130 and 870 Pa and at a fixed working distance of 9.5 mm. To control the sample temperature during the hydration experiments a water cooled peltier cooling stage was used.

With this instrumentation it is possible to create a defined relative humidity around the specimen by varying water vapor pressure in the microscope chamber and temperature of the peltier stage (= specimen temperature). For example, if the temperature is set to 5 °C and water vapor pressure is set to 499 Pa, according to the phase diagram of water a relative humidity of 55% results around the specimen (Figure 1).

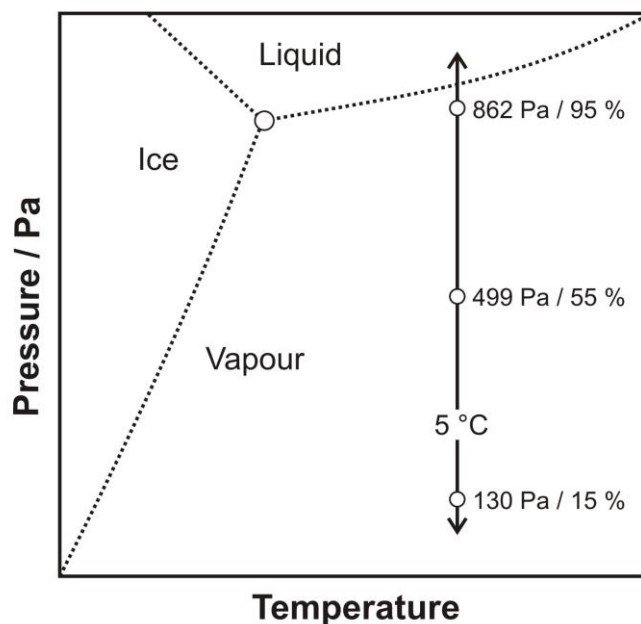


**Figure 1.** Sketch of the phase diagram of water and the used hydration path for isotherm measurements at 5 °C in the ESEM.

For isotherm measurements small amounts of clay powder were poured on the stainless steel sample holder and stage temperature and chamber pressure were set to 5 °C and 130 Pa, respectively. According to these parameters the relative humidity around the sample was 15 %. The specimen was left at these parameters at least for 15 minutes prior to the start of the experiments.

Swelling isotherms were measured by increasing the water vapor pressure in five steps from 130 Pa to 862 Pa, which correspond to relative humidities of 15, 35, 55, 75, 85, and 95 % respectively. At each step of pressure an image was taken after an equilibration time of 15 minutes. The last step of the hydration cycle at 862 Pa (95 % RH) was used as the first step of the dehydration cycle. Then the chamber pressure was decreased via the same five steps as in the hydration cycle until the starting conditions were achieved (130 Pa, 15 % RH). The sample temperature was always kept constant at 5°C.

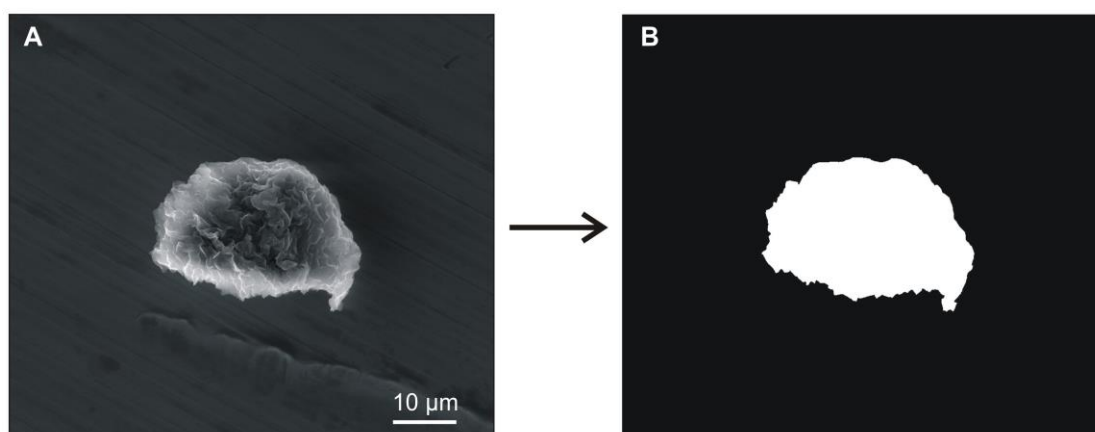


**Figure 2.** Digital image analysis of the clay images. A) ESEM image, B) binary image of the selected aggregate, obtained from the image analysis done with the ImageJ software.

For digital image analysis the open source software ImageJ was used (Rasband 2015). Bentonite aggregates with diameters between 30 and 50  $\mu\text{m}$  were selected for surface area measurements. The selected ESEM-images were converted to 8-bit and covered 1024 x 943 pixels. The area of interest (AOI) was isolated by applying a grey level threshold (Figure 2). Therefore, ImageJ considered a grey level range of 0-255 for all area measurements. Then the increase in surface area was calculated from the following equation:

$$\text{Swelling (\%)} = ((A_h - A_0) / A_0) \times 100 \quad (1)$$

Where  $A_h$  represents the surface area ( $\mu\text{m}^2$ ) of the hydrated sample and  $A_0$  represents the initial surface area ( $\mu\text{m}^2$ ) of the dry sample at 5 °C and 15 % RH. The data are displayed as areal expansion (swelling %) versus relative humidity at a fixed temperature and therefore can be indicated as isotherms.

### 3. Results

The changes in morphology of the bentonite aggregate during hydration are shown in Figure 3. The aggregate size remarkably increased with increasing humidity and also the typical rough smectite morphology changed considerably. An overlay image of the isolated AOI's illustrates the swelling process.

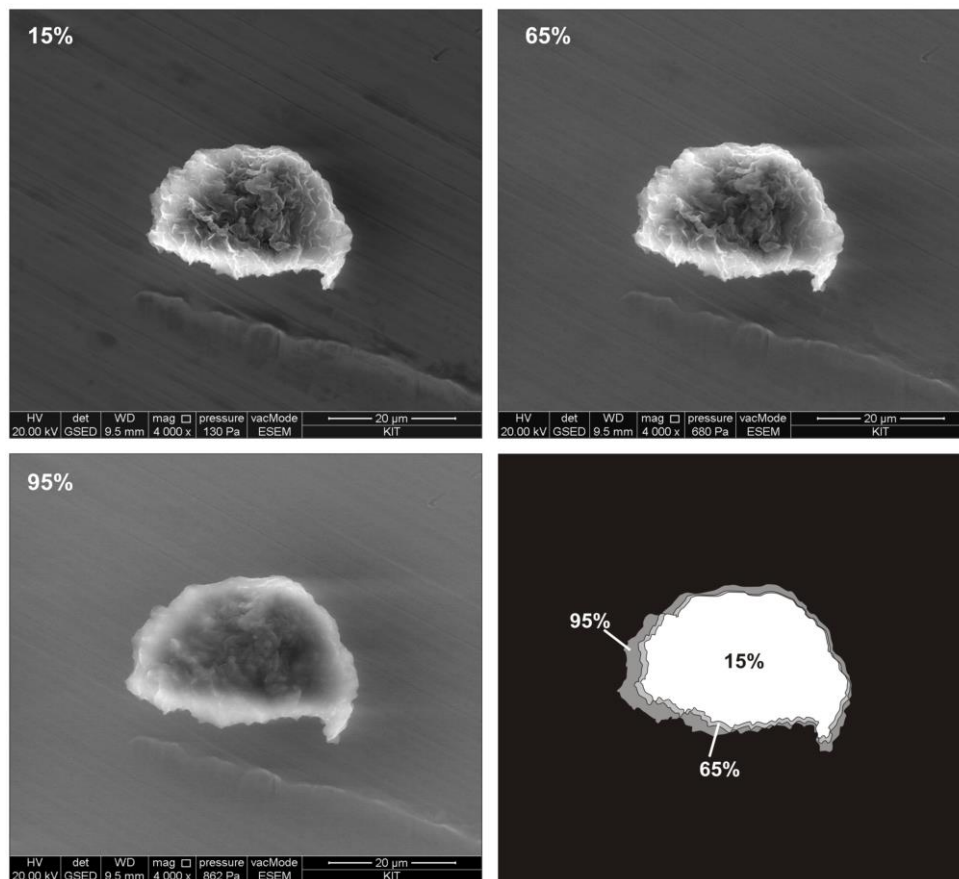


**Figure 3.** ESEM observation of FEBEX bentonite aggregate at relative humidities of 15, 65 and 95% respectively, showing remarkable changes in morphology. The overlay of binary images illustrates the swelling process.

The water adsorption isotherm of Na-Febex at 5 °C is displayed in Figure 4a. The swelling rates are very low at the beginning of the experiment. Not till relative humidities of 55 % the changes in particle morphology are clearly visible. The swelling finally increases exponentially at high humidities above 75 %. The dehydration path proceeds at slightly higher swelling percentages with decreasing relative humidities. In gas adsorption (BET-) measurements of smectites similar types of hysteresis are observed. There, this kind of hysteresis loop is called type H3, and is typical for plate-like particles giving rise to slit shaped pores (e.g. Sing et al. 1985).

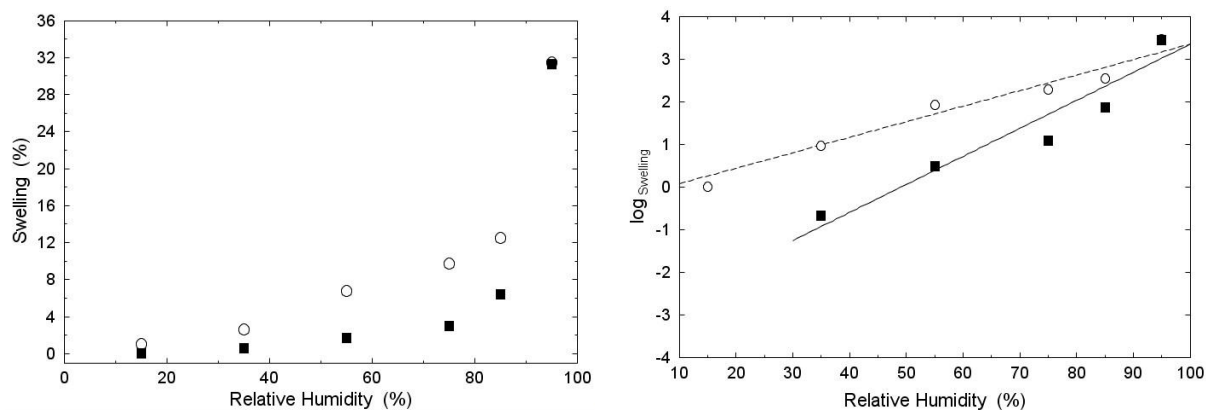


**Figure 4.** a) Measured isotherms of Na-FEBEX bentonite at 5 °C. Black squares: hydration path, white circles: dehydration path. b) Logarithmic plot of swelling vs. relative humidity representing a first order reaction of the hydration process with hindered dehydration ( $t_{\text{equil}} = 15$  min.).

A logarithmic representation of the swelling data is shown in Figure 4b. The measured data were fitted with a linear function. The slope of the hydration path ( $0.061 \pm 0.01$ ,  $R^2 = 0.914$ ) is larger than the one determined for the dehydration ( $0.036 \pm 0.004$ ,  $R^2 = 0.967$ ). Thus, hydration and dehydration can be assigned to a first order reaction, where the water availability is the driving force. Furthermore, the hydration exhibits a more pronounced dependency on the value of the relative humidity, than on the reverse action.

Similar behavior was observed by several authors using different techniques. But its interpretation still is under discussion. From XRD data, the hindered desorption was attributed to a decreased entropy (Fu et al. 1990) or to geometrical factors like changes in particle arrangement or interlayer distances (Cases et al. 1992). In addition, based on Monte Carlo simulations Tompsett et al. (2005) suggested network effects and cavitation phenomena for wide hysteresis loops in mesoporous materials.

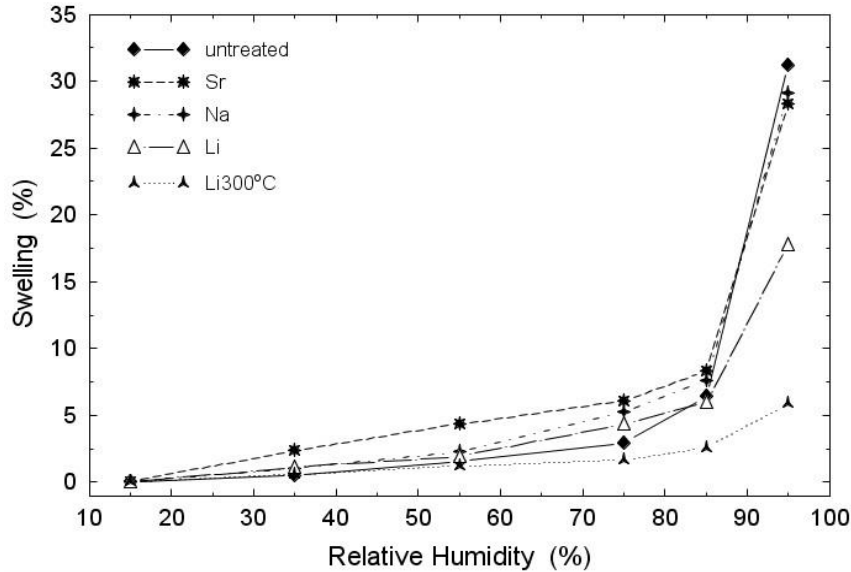


**Figure 5.** Comparison of the water adsorption isotherms of Na-, Li-, Li300- and Sr-exchanged bentonite vs. the untreated raw-material.

Hydration experiments with various cation exchanged bentonite samples (Figure 5) did not yield as many differences as reported by earlier studies (e.g. Keren and Shainberg 1975).

Untreated, Na- and Sr-exchanged samples swell to a similar maximum (max. swelling 29 and 28 %), while the swelling of Li-exchanged bentonite was slightly lower (max. swelling 18 %). Apart from that, the shapes of the hydration paths are very similar. In the layer charge reduced Li-sample (Li300 °C) the migration of water molecules into the interlayer is hindered, thus it swelled only to 6 %. This behavior has two reasons: First, the heat treatment leads to the migration of the lithium cations into the ditrigonal cavities of tetrahedral sheet, resulting in both a reduction of layer charge and the amount of interlayer cations. Secondly, this causes a collapse of the interlayer sheet to an illite-like d-spacing (e.g. Pálková et al. 2003).

The behavior of the untreated sample was similar to that of the Na- and Sr-samples with a slightly higher maximum swelling (31 %), which is related to a mixed cation occupancy of its interlayers (Na, Ca). Beyond that, the Sr-saturated bentonite showed a significantly higher swelling already at low relative humidities compared to the other samples. This can be assigned to the much higher hydration energy of divalent cations like Strontium ( $\Delta H_h^\circ = -1415$  kJ/mol) compared to alkali metals like Lithium or Sodium ( $\Delta H_h^\circ = -499$  and  $-390$  kJ/mol) (Wiberg et al. 2007). Bol et al. (1970) suggested, that divalent cations form two clear-cut hydration shells. This increases the hydration force within the clay interlayers, and results in large water spheres around the cation (Keren and Shainberg 1975). Nevertheless, the effect of the kind of interlayer cation on the swelling behavior of the clay aggregates was not as pronounced as it was discussed by earlier studies (e.g. Keren and Shainberg 1975).

#### 4. Conclusions and future work

The results of our study showed, that environmental scanning electron microscopy coupled with digital image analysis allowed for the in-situ observation and measurement of the swelling behavior of Febex bentonite in the range between 14 % and 95 % relative humidity and will be published in more detail in Friedrich et al. (2015).

Now, this technique will be used to investigate the swelling behavior of compacted bentonite samples. Also a comparison of the obtained data to the hydration behavior of other bentonites like MX80 or to synthetic smectites is planned.

## 5. References

Bol W., Gerrits G.J.A., van Panthaleon van Eck C.L. (1970) The hydration of divalent cations in aqueous solution. An X-ray investigation with isomorphous replacement. *Journal of Applied Crystallography*, **3**, 486–492.

Carrier B., Wang L., Vandamme M., Pellenq R., Bornert M., Tanguy A., Van Damme H. (2013). ESEM Study of the Humidity-Induced Swelling of Clay Film. *Langmuir*, **29**, 12823–12833.

Cases J.M., Bérend I., Besson G., Francois M., Uriot J.P., Thomas F., and Poirier J.E. (1992) Mechanism of adsorption and desorption of water vapor by homoionic montmorillonite. 1. The sodium-exchanged form. *Langmuir*, **8**, 2730–2739.

Donald A.M. (1998) Environmental scanning electron microscopy for the study of 'wet' systems. *Current Opinion in Colloid & Interface Science*, **3**, 143–147.

Fu M.H., Zhang Z.Z., and Low P.F. (1990) Changes in the properties of a montmorillonite-water system during the adsorption and desorption of water: hysteresis. *Clays and Clay Minerals*, **38**, 485–492.

Keren R., and Shainberg I. (1975) Water vapor isotherms and heat of immersion of Na/Ca-montmorillonite systems I: homoionic clay. *Clays and Clay Minerals*, **23**, 193–200.

Montes-H G., Duplay J., Martinez L., and Mendoza C. (2003) Swelling/shrinkage kinetics of MX80 bentonite. *Applied Clay Science*, **22**, 279–293.

Pálková H., Madejová J., Righi D. (2003) Acid dissolution of reduced-charge Li- and Ni-montmorillonites. *Clays and Clay Minerals*, **51**, 133–142.

Rasband W. (2015) ImageJ 1.48v. Developed at National Institutes of Health, USA. <http://imagej.nih.gov/ij>.

Sing K.S.W., Everett D.H., Haul R, Moscou L., Pierotti R., Rouquerol J., and Siemieniewska T. (1985) Reporting physisorption data for gas/solid systems with special reference to the determination of surface area and porosity. *Pure and Applied Chemistry*, **57**, 603–619.

Tompsett G.A., Krogh L., Griffin D.W., and Conner W.C. (2005) Hysteresis and scanning behavior of mesoporous molecular sieves. *Langmuir*, **21**, 8214–8225.